THE JOURNAL OF PHYSICAL CHEMISTRY C

Article

pubs.acs.org/JPCC

Li Ion Dynamics in a $LiAlO_2$ Single Crystal Studied by ^7Li NMR Spectroscopy and Conductivity Measurements

Sylvio Indris,*[,†] Paul Heitjans,[‡] Reinhard Uecker,[§] and Bernhard Roling[∥]

[†]Institute of Nanotechnology, Karlsruhe Institute of Technology, P.O. Box 3640, 76021 Karlsruhe, Germany

[‡]Institut für Physikalische Chemie und Elektrochemie, Leibniz Universität Hannover, Callinstraße 3-3A, 30167 Hannover, Germany

[§]Institut für Kristallzüchtung, Max-Born-Straße 2, 12489 Berlin, Germany

[∥]Fachbereich Chemie, Philipps-Universität Marburg, Hans-Meerwein-Straße, 35032 Marburg, Germany

ABSTRACT: Dynamics of lithium ions in solid materials is a key parameter for applications such as electrode materials for lithium ion batteries. The Li diffusion in single crystalline γ-$LiAlO_2$ was studied with temperature-dependent ^7Li NMR spectroscopy and conductivity measurements. The NMR measurements include a detailed study of the temperature dependence of static spectra and spin−lattice relaxation rate measurements. A combination of these methods allowed us to study diffusion coefficients over a range of more than seven decades. The range covered was 10^{-20} to 10^{-13} m^2 s^{-1} corresponding to jump rates between 10^0 and 10^7 s^{-1}. An activation energy of about 1 eV was found. The hopping between crystallographically equivalent Li sites was explicitly verified by coalescence of quadrupole satellites in the NMR spectra.

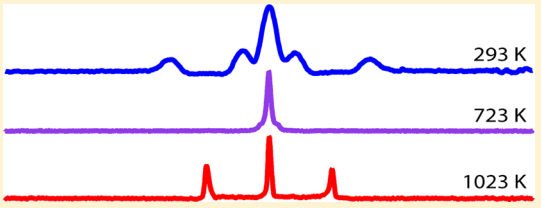

INTRODUCTION

γ-$LiAlO_2$ crystallizes in the tetragonal space group $P4_12_12$. A unit cell of this crystal contains four formula units and has lattice parameters a = 5.1687 ± 0.0005 Å and c = 6.2679 ± 0.0006 Å.[1] There are four chemically equivalent but magnetically inequivalent sites for the Li as well as for the Al atoms. $LiAlO_2$ is used as a substrate material for epitaxial growth of III−V semiconductors like GaN.[2] The stability of such systems during processing and operation will depend on lithium diffusion in the substrate and from the substrate into the semiconducting films. Furthermore, $LiAlO_2$ is used as a coating in Li electrodes[3] and as an additive in composite Li electrolytes.[4] Again, Li diffusion is a crucial process for these applications. $LiAlO_2$ is also considered as a candidate material for tritium breeder or fusion reactors.[5] In this case, tritium release and diffusion will depend on lithium diffusion in this material. Therefore, molecular dynamics simulation had been carried out, which predicted a Li diffusion coefficient of 2.8×10^{-11} m^2/s at 600 K and an activation energy of 0.5 eV.[5] First, NMR measurements were performed on powder samples to investigate the local electronic structure at the Al sites[6] and ^7Li T_1 relaxation times.[7] The electronic structure in a single crystal of $LiAlO_2$, being identical to the one used here, was studied via the orientation dependence of ^7Li NMR spectra.[8] From this, the complete electric field gradient (EFG) tensor was determined for the Li positions. In this study, we present investigations of the Li dynamics in a γ-$LiAlO_2$ single crystal. For this purpose, we performed temperature-dependent NMR spectroscopic studies as well as measurements of the ionic conductivity. NMR is a versatile tool to study the dynamics of, for example, Li ions in condensed matter over a large range of correlation times.[9] We examined the temperature dependence of ^7Li NMR relaxation rates and of static ^7Li NMR spectra. The latter one comprises the motional narrowing of the central transition as well as the coalescence of quadrupolar satellites.

SAMPLE PREPARATION

$LiAlO_2$ single crystals were grown using the Czochralski technique with radiofrequency induction heating. During the growth of these crystals, strong selective evaporation of Li_2O might occur from the melt as well as from the crystal. Its suppression required particular temperature gradients extremely different from the standard ones for oxides. The found conditions allow the growth of $LiAlO_2$ crystals with a diameter of up to 50 mm, a length of 80 mm, and good perfection. The starting melt was prepared from predried $^7Li_2CO_3$ (99.99%) and Al_2O_3 (99.99%) powders, which were mixed in the stoichiometric ratio and sintered subsequently. Because of the high melting temperature of about 2000 K, both the crucible and the active afterheater were made of iridium. The pulling rate was 1.5 mm h^{-1}, and the rotation rate was 10 min^{-1}. Flowing argon was used as the growth atmosphere, and the crystals were pulled along the [110] orientation.

EXPERIMENTAL SETUP

^7Li NMR measurements of static lineshapes as well as of spin−lattice relaxation rates T_1^{-1} were measured on a Bruker MSL 100 spectrometer in combination with a tunable cryomagnet (0−7T) and a home-built probe. Measurements were

Received: May 3, 2012
Revised: June 14, 2012
Published: June 14, 2012

   dx.doi.org/10.1021/jp3042928 | J. Phys. Chem. C 2012, 116, 14243−14247

performed at a resonance frequency of 77.8 MHz and temperatures between 300 and 1100 K. Lineshapes were acquired with a solid-echo pulse sequence to avoid dead time effects during data acquisition, and for the relaxation time measurements, a saturation-recovery pulse sequence was used to reduce the experiment duration.[10] The $\pi/2$ pulse length was typically 3 μs, and the repetition time for the solid-echo experiments was set to $5 \times T_1$.

To study the electrical conductivity in [001] and [110] directions, platinum electrodes were sputtered on the respective surfaces of the single crystals. The conductivity measurements were carried out by using a Novocontrol alpha-S high-resolution impedance analyzer in a frequency range from 1 mHz to 3 MHz and in a temperature range from 423 to 623 K. The dc conductivities were extracted from the low-frequency plateaus of the conductivity spectra.

RESULTS

Figure 1a shows ^{7}Li NMR spectra of the $LiAlO_2$ single crystal for temperatures between 293 and 1023 K. Because ^{7}Li has a nuclear spin $I = 3/2$, each Li site appears as a triplet pattern in the ^{7}Li NMR spectrum. One triplet pattern consists of a central line corresponding to the transition $|+1/2\rangle \leftrightarrow |-1/2\rangle$ and quadrupolar satellites corresponding to the transitions $|+3/2\rangle \leftrightarrow |+1/2\rangle$ and $|-1/2\rangle \leftrightarrow |-3/2\rangle$. The spectra show more than one satellite pair at low temperatures because the Li sites are not equivalent any more since the symmetry at the site of the Li nuclei is broken by the magnetic field. The single crystal was oriented such that the [110] direction was parallel to the direction of the external magnetic field. This orientation was chosen because at low temperatures it gives a spectrum with a central line at the Larmor frequency ($\nu - \nu_L = 0$) and two pairs of well-resolved quadrupolar satellites at ± 12 and ± 46 kHz, each of them corresponding to two of the four crystallographically equivalent Li sites per unit cell. The dependence of the spectral line shape on the orientation of the single crystal was studied in detail earlier by us.[8] From this, the quadrupole coupling constant $C_q = e^2Qq/h = 115.1 \pm 0.6$kHz and the asymmetry parameter $\eta_Q = 0.69 \pm 0.01$ had been determined. Q is the quadrupole moment of the nucleus, and q is the electric field gradient. The quadrupole moment of ^{7}Li is $Q = -40.1$ mb.[11]

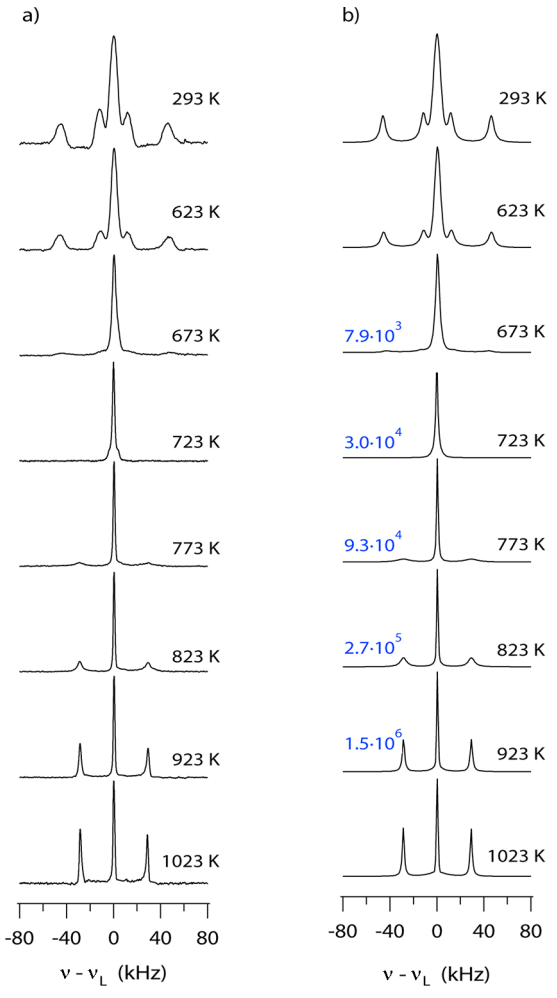

Figure 1. (a) ^{7}Li NMR lineshapes of a $LiAlO_2$ single crystal with B|| [110] measured at temperatures between 293 and 1023 K and a Larmor frequency ν_L of 77 MHz. (b) ^{7}Li NMR lineshapes calculated as described in the text. The extracted jump rates are given in blue.

When the temperature is increased, starting from room temperature, the following features are observed, which clearly reflect the onset of Li motion with correlation rates of some 10 kHz. Between 293 and 623 K, no major changes are observed. At 673 K, the two pairs of quadrupole satellites are strongly broadened and hardly visible anymore, and they disappear completely at 723 K. At 773 K, a new, broad, single pair of quadrupole satellites appears at ± 29 kHz, that is, exactly in the middle between the positions of the initial two pairs of satellites. At even higher temperatures, these satellites show a narrowing with increasing temperature. This characteristic coalescence of NMR lines due to the onset of motion of the underlying nuclei occurs when the jump rate of the atoms reaches the difference of the resonance frequencies (about 34 kHz in this case). Because the quadrupole satellites are sensitive to the electric field gradient in the direction of the magnetic field, in the present case, we are able to observe jumps between crystallographically equivalent sites by using a single crystal.

The coalescence of two NMR lines with resonance frequencies $\pm \delta$ due to hopping of the atoms between the two sites can be described by[12]

$$I_{coal}(\omega) = \mathrm{re}\{\mathbf{W}\cdot\mathbf{A}^{-1}\cdot\mathbf{1}\} \tag{1}$$

with

$$\mathbf{A} = \mathrm{i}(\boldsymbol{\omega} - \omega\mathbf{E}) + \boldsymbol{\Pi} \tag{2}$$

$\mathbf{E}$ is the unit matrix

$$i\boldsymbol{\omega} = \begin{pmatrix} \mathrm{i}\delta - \dfrac{1}{\tau_i} & 0 \\ 0 & -\mathrm{i}\delta - \dfrac{1}{\tau_i} \end{pmatrix} \tag{3}$$

is the diagonal matrix whose eigenvalues are the resonance frequencies and

$$\boldsymbol{\Pi} = \begin{pmatrix} -\Omega & \Omega \\ \Omega & -\Omega \end{pmatrix} \tag{4}$$

describes the probabilities $\Omega = \tau^{-1}$ per unit time to jump from one frequency to the other. The term $1/\tau_i$ describes the intrinsic linewidths at low temperatures,

dx.doi.org/10.1021/jp3042928 | J. Phys. Chem. C 2012, 116, 14243−14247

$$\mathbf{W} = \begin{pmatrix} \frac{1}{2} \\ \frac{1}{2} \end{pmatrix} \quad (5)$$

comprises the occupancies of the different sites and

$$\mathbf{1} = \begin{pmatrix} 1 \\ 1 \end{pmatrix} \quad (6)$$

Equation 1 is independent of the fact whether the resonance frequencies stem from the central transition $|+1/2\rangle \leftrightarrow |-1/2\rangle$ or from a quadrupolar transition $|\pm 3/2\rangle \leftrightarrow |\pm 1/2\rangle$. It can be used to describe the coalescence of the quadrupolar satellites on each side of the central line separately. To describe the complete symmetric line shape comprising the multiple triplet patterns consisting of the central resonance line and the quadrupolar satellites, we used the expression

$$I_{\mathrm{coal}}(\omega + H) + I_{\mathrm{central}}(\omega) + I_{\mathrm{coal}}(\omega - H) \quad (7)$$

The first term describes the coalescence of the quadrupolar satellites on the left side, the second term describes the central line, and the third term describes the coalescence of the quadrupolar satellites on the right side of the spectrum. H is the parameter describing the center of gravity of the quadrupolar satellites on each side of the spectrum. For the central transition $I_{\mathrm{central}}(\omega)$, we used the sum of a Gaussian and a Lorentzian line shape. The results of the calculated lineshapes are shown in Figure 1b in comparison with the experimental results. In the case where the magnetic field is pointing along the [001] direction of the single crystal, all four Li ions per unit cell are equivalent,[8] and only one pair of quadrupole satellites is visible over the complete temperature range.

Besides the coalescence of the quadrupolar satellites, a narrowing of the central line can be observed starting at about 600 K. This is shown in detail in Figure 2 where the line width

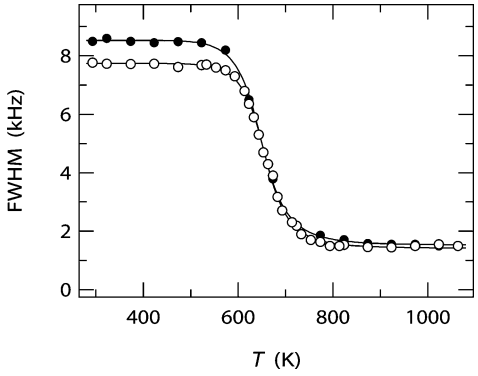

Figure 2. ^{7}Li NMR linewidths vs temperature for the central resonance measured at a frequency of 77 MHz on a $LiAlO_2$ single crystal with $B\|[110]$ (○) and $B\|[001]$ (●). The solid lines show the results of a fit according to eq 8.

of the central line is plotted as a function of temperature for two different orientations of the single crystal. As described above for $B\|[001]$, all four Li ions per unit cell are equivalent,[8] and only one pair of quadrupole satellites is visible for the complete temperature range. In this case, no coalescence of quadrupole satellites occurs, and the satellites show exactly the same narrowing as the central transition. Different ad hoc formulas exist to describe the line width $\Delta\nu$ of the central transition as a function of the correlation time τ_c[12−16] and to extract jump rates and activation energies for the Li motion. We used the implicit expression

$$(\Delta\nu)^2 = (\Delta\nu'')^2 + (\Delta\nu')^2 \cdot \frac{2}{\pi} \cdot \tan^{-1}(\alpha \cdot \Delta\nu \cdot \tau_c) \quad (8)$$

by Abragam,[12] where $\Delta\nu$ is the line width at a given temperature T [for simplicity, we used the full width at half-maximum (fwhm) instead of the second moment $\Delta\nu$], α is a constant of the order of unity depending on the exact line shape (here chosen to be equal to one), and ν' and ν'' describe the plateau values at very low and high temperatures, respectively. It can be seen at low temperatures, in the so-called rigid-lattice regime, that the line width is somewhat larger for $B\|[001]$ than for $B\|[110]$, reflecting a stronger dipolar coupling along the [001] direction.

The temperature dependence of the NMR spectra gives access to ionic motion with correlation rates of the order of the width of the spectral features, that is, some 10 kHz. Another NMR technique to study dynamics in condensed matter is the measurement of spin−lattice relaxation rates T_1^{-1}.[9] This method is sensitive to motion with correlation rates of the order of the Larmor frequency, that is, about 100 MHz. Figure 3 shows the

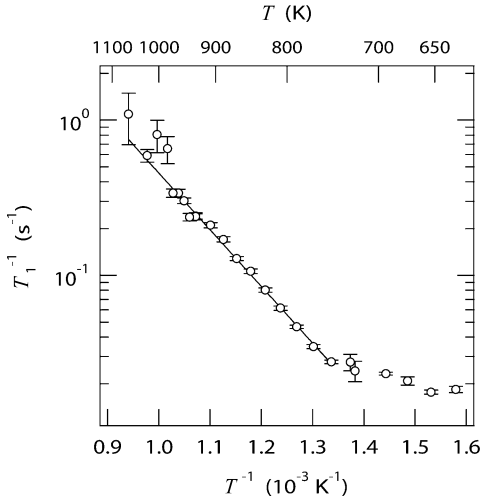

Figure 3. ^{7}Li NMR relaxation rate T_1^{-1} measured at a frequency of 77 MHz on a $LiAlO_2$ single crystal with $B\|[110]$.

temperature dependence of T_1^{-1} at temperatures between 633 and 1063 K. The measurements were done with the magnetic field aligned parallel to the [110] direction. At temperatures below 750 K, only a weak temperature dependence is visible. At higher temperatures, $T_1^{-1}(T)$ shows Arrhenius behavior, which indicates that T_1^{-1} is dominated by Li hopping in this regime. Assuming isotropic, Markovian hopping of the Li ions and predominantly quadrupolar relaxation, the relaxation rate of nuclei with $I = 3/2$ can be described by the expression[12,17]

$$\frac{1}{T_1} = \frac{2\pi^2}{25} \cdot C_q^2 \cdot \left(1 + \frac{\eta_Q^2}{3}\right) \cdot \left[\frac{\tau_c}{1 + \omega^2\tau_c^2} + \frac{4\tau_c}{1 + 4\omega^2\tau_c^2}\right] \quad (9)$$

Using the quadrupole coupling constant C_q and the asymmetry parameter η_Q determined earlier,[8] this expression can be used to transform the relaxation rates into motional correlation rates τ_c^{-1}. Apart from a factor of the order of unity

dx.doi.org/10.1021/jp3042928 | J. Phys. Chem. C 2012, 116, 14243−14247

(here chosen to be equal to one), these can be identified with the average jump rates τ^{-1} of the ions. The results will be discussed below in the Discussion.

The average jump rates τ^{-1} can be used to determine the diffusion coefficient D^{T} of the Li ions via the Einstein–Smoluchowski equation[18,19]

$$D^{T} = f \cdot \frac{l^2}{6\tau} \tag{10}$$

l is the jump distance that can be taken from the shortest Li–Li distance in the crystal structure (3.091 Å in this case) if a vacancy mechanism is assumed. f is the correlation factor that can be calculated if the diffusion mechanism is known.[9,20,21] Here, we use f = 1, which corresponds to completely uncorrelated motion of the Li ions.

Besides the different NMR techniques, an alternative approach to determine the diffusion coefficient of the Li ions is to measure the ionic conductivity σ_{dc} and calculate the diffusion coefficient via the Nernst–Einstein-equation

$$D^{T} = H_R \cdot \frac{k_B T}{N q_c^2} \cdot \sigma_{dc} \tag{11}$$

k_B is the Boltzmann constant, T the temperature, N the number density of mobile Li ions (2.39×10^{28} m^{-3} for γ-$LiAlO_2$), and q_c is their charge. H_R is the Haven ratio, which comprises correlation effects in the movement of the ions and cases where motions of uncharged defects occur that do not contribute to the conductivity.[21−23] In case that only one defect species is present in the single crystalline material, H_R equals f, and eqs 10 and 11 can be used to calculate the Li jump rate $1/\tau$ from the conductivity σ_{dc}. Figure 4 shows the dc conductivity for the

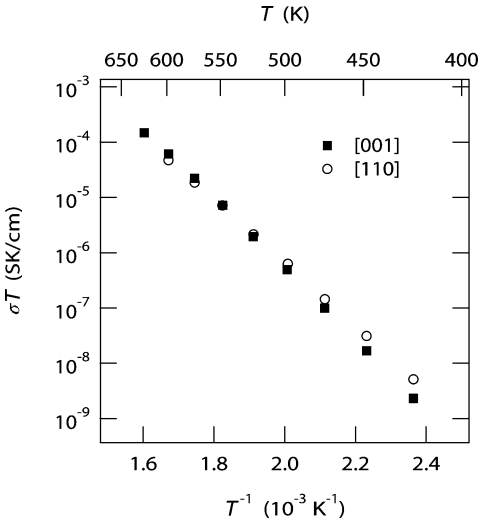

Figure 4. dc conductivity of a $LiAlO_2$ single crystal in [001] direction (■) and [110] direction (○) for temperatures between 423 and 623 K.

$LiAlO_2$ single crystal along the [110] and the [001] direction for temperatures between 423 and 623 K. The conductivity shows Arrhenius behavior in both cases and only slight differences between the two directions. The activation energies turned out to be 1.26 ± 0.01 eV and 1.14 ± 0.01 eV for the conductivity in the [001] and the [110] directions, respectively.

DISCUSSION

The results of the NMR as well as conductivity measurements have been used to calculate jump rates τ^{-1} for the motion of the Li ions. Altogether, the temperature range from 423 to 1023 K was covered. The resulting correlation rates, obtained from the NMR measurements with $B\|[110]$ and the conductivity data in the [110] direction, are shown in Figure 5. The corresponding

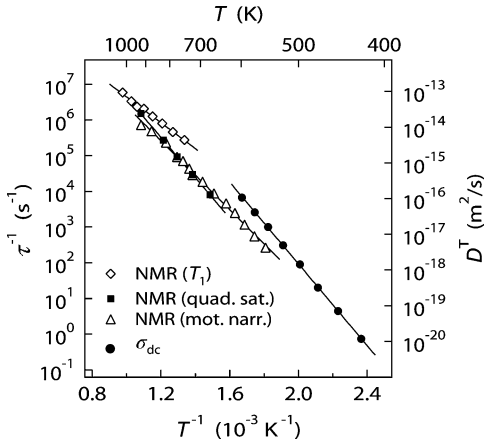

Figure 5. Jump rates τ^{-1} of the Li ions and the corresponding diffusion coefficients D^{T} vs inverse temperature. The data points were calculated from conductivity measurements (●), ^{7}Li NMR relaxation rates (◇), and the temperature dependence of static ^{7}Li NMR lineshapes. The latter one includes the motional narrowing of the central transition (△) and the coalescence of the quadrupolar satellites (■). In all cases, the NMR data for $B\|[110]$ and the conductivity data for the [110] direction were used.

data for the [001] direction give very similar results, except for the fact that no coalescence of the quadrupole satellites occurs; that is, only three data sets are available. The conductivity data (Figure 4) were first transformed to diffusion coefficients via eq 11, and from that, the jump rate was calculated via eq 10 using H_R = 1 and f = 1. For the NMR measurements, the correlation rates were extracted via eqs 1–7, 8, and 9 for the coalescence of the quadrupole satellites (Figure 1), the motional narrowing of the central transition (Figure 2), and the spin–lattice relaxation (Figure 3), respectively. The diffusion coefficient was then calculated via eq 10 (again using f = 1). D^{T} is also shown in Figure 5 (right ordinate) for the NMR as well as for the conductivity measurements. Overall, the four different data sets give a fair agreement. Each data set is fitted with an Arrhenius ansatz

$$\frac{1}{\tau} = \frac{1}{\tau_0} \cdot \exp\left(-\frac{E_A}{k_B T}\right) \tag{12}$$

which yields the activation energy E_A and the pre-exponential factor τ_0^{-1} for the Li motion. The results are summarized in Table 1. The T_1^{-1} data give a significantly smaller activation energy (0.7 eV) than the other measurements, which yield a consistent value of about 1 eV. Because the T_1^{-1} data include only the low-temperature flank of the diffusion-induced peak, this might hint at correlations in the motion of the Li ions and therefore to a vacancy mechanism.[9] This is corroborated by a dispersive region that is apparent at high frequencies in conductivity spectra (not shown here). Such a correlated motion can lead to deviations from the behavior expressed by eq 9 with a smaller apparent activation energy on the low-

dx.doi.org/10.1021/jp3042928 | J. Phys. Chem. C 2012, 116, 14243−14247

Table 1. Activation Energies E_A and Pre-exponential Factors τ_0 as Determined from Different NMR Techniques and Dc Conductivity Measurements[a]

method	E_A (eV)	τ_0 (s)
NMR (T_1)	0.72 ± 0.02	$(5.5 \pm 1.5) \times 10^{-11}$
NMR (mot. narr.)	0.96 ± 0.02	$(6.4 \pm 1.7) \times 10^{-12}$
NMR (quad. sat.)	1.12 ± 0.01	$(5.1 \pm 0.5) \times 10^{-13}$
σ_{dc}	1.14 ± 0.01	$(3.8 \pm 0.6) \times 10^{-14}$

[a]In all cases, the NMR data for $B \| [110]$ and the conductivity data for the [110] direction were used.

temperature flank of the diffusion induced maximum in T_1^{-1} (T^{-1}) than on the high-temperature flank (the latter one not being accessible in our experiments).[9]

The jump rates determined from the conductivity measurements are somewhat higher than the ones obtained from the NMR results. One possible explanation is that the real jump length is larger than the one assumed in our calculation, that is, the shortest Li−Li distance within the crystal structure. For example, instead of a direct jump from one tetrahedral site to the next, an octahedral interstitial site might be involved as a transition site in the elementary jump process. Another explanation could be a Haven ratio smaller than the correlation factor ($H_R < f$), which might hint to additional contributions to the overall conductivity that do not contribute to Li diffusion.[22,23]

Combining different NMR techniques and conductivity measurements, it was possible to determine motional correlation rates over a range of more than seven decades. The conductivity measurements show only a weak orientation dependence. A detailed analysis of the temperature dependence of the NMR line shape measurements on this single crystal was possible by making use of earlier studies on the orientation dependence of ^{7}Li NMR spectra.[8] The exact diffusion pathway is not clarified yet. The Li ions could jump from one regular tetrahedral site to the next tetrahedral site via octahedrally coordinated interstitial sites or via channels in the crystal structure. The exact diffusion pathway will be studied in future experiments by high-temperature neutron diffraction and molecular dynamics simulations.

CONCLUSION

We investigated the Li ion dynamics in a $LiAlO_2$ single crystal. The long-range Li diffusion could be studied by conductivity measurements. ^{7}Li NMR measurements are sensitive specifically to the dynamics of the Li ions. This was made use of by applying different NMR techniques including measurements of the spin−lattice relaxation rates and the temperature dependence of static spectra. The coalescence of quadrupole satellites was used to explicitly observe the hopping between crystallographically equivalent sites in a single crystal.

AUTHOR INFORMATION

Corresponding Author

*Tel: +49-721-608-28312. Fax: +49-721-608-26368. E-mail: sylvio.indris@kit.edu.

Notes

The authors declare no competing financial interest.

ACKNOWLEDGMENTS

We are grateful to the Deutsche Forschungsgemeinschaft for financial support.

REFERENCES

(1) Marezio, M. *Acta Crystallogr.* **1965**, *19*, 396.
(2) Waltereit, P.; Brandt, O.; Ploog, K. H. *Appl. Phys. Lett.* **1999**, *75*, 2029.
(3) Cao, H.; Xia, B.; Zhang, Y.; Xu, N. *Solid State Ionics* **2005**, *176*, 911.
(4) Dissanayake, M. A. K. L. *Ionics* **2004**, *10*, 221.
(5) Jacobs, J.-P.; San Miguel, M. A.; Alvarez, L. J.; Giral, P. B. *J. Nucl. Mater.* **1996**, *232*, 131.
(6) Müller, D.; Gessner, W.; Scheler, G. *Polyhedron* **1983**, *2*, 1195.
(7) Matsuo, T.; Ohno, H.; Noda, K.; Konishi, S.; Yoshida, H.; Watanabe, H. *J. Chem. Soc., Faraday Trans. 2* **1983**, *79*, 1205.
(8) Indris, S.; Heitjans, P.; Uecker, R.; Bredow, T. *Phys. Rev. B* **2006**, *74*, 245120.
(9) Heitjans, P.; Schirmer, A.; Indris, S. In *Diffusion in Condensed Matter—Methods, Materials, Models*; Heitjans, P., Kärger, J., Eds.; Springer: Berlin, 2005; pp 367−415.
(10) Fukushima, E.; Roeder, S. B. W. *Experimental Pulse NMR*; Addison-Wesley: Reading, MA, 1981.
(11) Pyykkö, P. *Mol. Phys.* **2001**, *99*, 1617.
(12) Abragam, A. *The Principles of Nuclear Magnetism*; Oxford University Press: Oxford, 1999.
(13) Gutowsky, H. S.; Pake, G. E. *J. Chem. Phys.* **1950**, *18*, 162.
(14) Waugh, J. S.; Fedin, E. I. *Sov. Phys. Solid State* **1963**, *4*, 1633.
(15) Hendrickson, J. R.; Bray, P. J. *J. Magn. Reson.* **1973**, *9*, 341.
(16) Xia, Y.; Machida, N.; Wu, X.; Lakeman, C.; van Wüllen, L.; Lange, F.; Levi, C.; Eckert, H. *J. Phys. Chem. B* **1997**, *101*, 9180.
(17) Spiess, H. W. In *Dynamic NMR Spectroscopy*; Diehl, P., Fluck, E., Kosfeld, R., Eds.; Springer: Berlin, 1978; Vol. *15*; pp 55−214.
(18) Einstein, A. *Ann. Phys., Lpz.* **1905**, *17*, 549.
(19) von Smoluchowski, M. *Ann. Phys., Lpz.* **1906**, *21*, 756.
(20) Claire, A. D. L. In *Physical Chemistry—An Advanced Treatise*; Eyring, H., Henderson, D., Jost, W., Eds.; Academic: New York, 1970; Vol. *10*; pp 261−330.
(21) Heitjans, P.; Indris, S. *J. Phys.: Condens. Matter* **2003**, *15*, R1257.
(22) Bénière, F. In *Physics of Electrolytes*; Hladik, J., Ed.; Academic Press: London, 1972.
(23) Murch, G. E. *Solid State Ionics* **1982**, *7*, 177.

NOTE ADDED AFTER ASAP PUBLICATION

This article was published ASAP on June 28, 2012. Figures 1, 3, 4, and 5 have been modified. The correct version was published on July 12, 2012.